Pergamon

0301-9322(94)00094-8

Int. J. Multiphase Flow Vol. 21, No. 4, pp. 649–665, 1995

0301-9322/95 $9.50 + 0.00

ANALYSIS OF HIGH DENSITY GAS–SOLIDS STRATIFIED PIPE FLOW

J. HONG and Y. TOMITA†

Department of Mechanical Engineering, Kyushu Institute of Technology, Kitakyushu 804, Japan

(Received 25 April 1994; in revised form 15 December 1994)

Abstract—This paper presents an improved model for high density gas–solids stratified pipe flow, in which the particle–particle interactions between the suspension and the sliding bed are taken into account by introducing suspended particle distribution coefficients, and examines the transition of stable stratified flow. Furthermore, phase diagram, distribution of suspended particles, solids concentration and velocity are predicted by the present model. It is found that particles begin to drop out of the gas phase at the theoretical saltation point at which the velocity is higher than that at the Rizk saltation point. The turning point in a diagram of dimensionless sliding bed height versus Froude number is close to the Rizk saltation point, while the Muschelknautz & Wojahn critical point is reasonable as the lower limit of the stable stratified flow of fine particles. In the phase diagram, the minimum pressure-drop point is to the left of the Rizk saltation point. Solids concentration in stable stratified flow is much lower than that of its loosely packed bed. In suspension, at most 25% of suspended particles saltate over the surface of the sliding bed. Velocity ratios of solids-to-actual gas and sliding bed-to-superficial gas increase with Froude number except at very low Froude numbers.

Key Words: gas–solids stratified flow, sliding bed, saltation velocity, critical velocity, particle–particle interaction

1. INTRODUCTION

Different gas–solids flow regimes occur when the gas velocity reduces gradually in a horizontal pneumatic system. At the two extreme cases, dilute gas–solids suspensions and dense phase plug flow operated at high and low velocities, respectively, have been widely and successfully applied in industry over the past several decades on the basis of a number of fundamental experiments and theoretical works (Doig 1975; Soo 1980; Bohnet 1985; Konrad 1986; Klinzing *et al.* 1987; Marcus *et al.* 1990). However, only a few studies have been conducted for gas–solids stratified flows consisting of a suspension layer and a layer of dense sliding bed, which is the transitional region between the suspended flow and plug (Bohnet 1965; Muschelknautz & Krambrock 1969; Muschelknautz & Wojahn 1973; Wirth & Molerus 1981; Lucht & Soo 1990; Hong 1992a; Hong *et al.* 1993).

Saltation velocity, which is defined as the gas velocity where the particle begins to separate from the gas phase and slides or rolls along the bottom of the pipe, may be treated as the minimum transport velocity of dilute-phase suspensions as well as the upper boundary of high density gas–solids stratified flow and estimated by various correlations. Generally, there are two empirical approaches to determine this velocity: visual observation and measurements of minima in pressure drop–velocity phase diagrams with the solids/gas flowrate ratio or solids mass flowrate as a parameter although it is recognized that the minima may be changed for different parameters. Visual inspection is direct but usually full of subjectivity. For the latter, Jones & Leung (1978) compared the eight published correlations with the experimental data obtained in small-scale units at low pressure and then recommended the formula of Rizk (1976) to predict saltation point in the light of accuracy and simplicity. Recently, Geldart & Ling (1992) found that Rizk's formula is also reasonable for high pressure conveying of fine coal in a pilot-scale unit. Considering particles slide on the bottom of the pipe in the vicinity of saltation velocity, Ochi & Ikemori (1978) and Ochi (1991) reported two expressions including the wall friction factor of solids for the saltation point of a coarse particle. In these empirical correlations, many variables in the solids properties and

†To whom correspondence should be addressed.

system operating parameters were considered, however, the applicability of the correlations is still limited in the sense of common use since the complicated transitional structure of stratified flow has been ignored (Molerus & Wirth 1991).

The lower boundary of stable stratified flow is called as the critical velocity which is defined as that prevailing at the appearance of the first unstable plug by Wirth & Molerus (1986). They found that safe conveying is possible with a gas velocity smaller than the saltation velocity depending on the characteristics of the blower employed (Wirth & Molerus 1981, 1986). Muschelknautz & Wojahn (1973) measured the critical velocity required for stable stratified flow of fine particles and found that the critical Froude number is determined only by the density ratio of the sliding bed (so-called strand) to the gas phase. Later, Wirth (1983) made the stability analysis of a coarse particle stratified flow in a broad velocity range and reached an approximate equation on the critical velocity allowing for the influence of properties of solids and operating parameters. Comparison of their experiments showed that this equation might be extended to fine particles, although in their derivation it was claimed to be valid only for coarse particles and the assumption that all the solids practically slide along the bottom of the pipe was adopted (Wirth & Molerus 1986).

Several theoretical models have been developed to predict the pressure drop in a gas–solids stratified pipe flow. Bohnet (1965) assigned the effect of wall friction exclusively to the particles in suspension and the effect of gravity to the solids in the sliding bed and proposed the pressure drop coefficient for solids which is reasonable for solids/gas flowrate ratios below 20–50. It was recognized that the shear force exerted on the surface of a sliding bed by the impact of suspended particles plays an important role in the motion of a sliding bed. Based on the force balance for the sliding bed of fine particles, Muschelknautz & Krambrock (1969) and Muschelknautz & Wojahn (1973) derived the total pressure drop which was mainly contributed by the friction of a sliding bed due to its gravity. Wirth & Molerus (1981) also analyzed the shear stress and frictional force exerted on a sliding bed of coarse particles to obtain the additional pressure drop by the solids. However, the detailed analysis of interaction between suspension and sliding bed is still lacking so that their predictions for pressure drop are far from reliable compared with the industrial data (Bohnet 1990). Recently, Hong *et al.* (1993) developed a model which accounts for the specific modes of interactions to overcome the shortcomings of the previous models since the impact and lift-off angles during the saltation of suspended particles are critically related to momentum transfer of saltating particles of sliding bed.

A similar process to the stratified pipe flow is the impact in aeolian saltation in the field of geology. Early observations of Bagnold (1941) and Chepil (1945) suggested that saltating particles lift off the surface of a stationary bed nearly vertically and then impact the surface at low angles between 10 and 16°. Later experimental measurements (Tsuchiya 1970; White & Schulz 1977; Nalpanis 1985) and theoretical simulations (Nalpanis 1985; White 1982; Rumpel 1985) for steady-state saltation showed that the lift-off angle is about 40° for uniform-sized sand and within 20–100° for non-uniform-sized sand and this angle might have been biased to be larger in the earlier work due to the difficulty of judging the trajectory of the saltating particle in the near-surface region. Whereas the impact angle was confirmed to be between 5 and 20° over a wide range of conditions (White & Schulz 1977; Rumpel 1985; Ungar & Haff 1987; Werner 1990) and the finer the particle, the smaller the angle (White 1986). Partially based on the experiments, a simple expression to correlate the average impact and life-off angles has been proposed by White & Schulz (1977) and seems also to be valid for stratified pipe flow (Hong 1992b). On the other hand, Rumpel (1985) reported that the impact of a successively saltating particle should augment the magnitude of its vertical velocity. In the two-dimensional simulations of Werner & Haff (1988), the vertical velocity amplification defined as the ratio of lift off to incident vertical velocity was found to strongly depend on and be inversely proportional to the impact angle and to be unity when the impact angle is 15°. Comparatively, the change of horizontal velocity before and after the collision with the surface is considerable. This introduces a possible supposition that the saltating particle elastically collides with the surface in the vertical direction.

The structure of the transition of a gas–solids stratified pipe flow has not been fully discussed until now, in spite of the analysis for the height of a sliding bed in a high density flow of fine particles (Muschelknautz & Krambrock 1969; Muschelknautz & Wojahn 1973; Hong *et al.* 1993)

or granular solids (Wirth & Molerus 1986) and for the velocity of a sliding bed (Bohnet 1965; Muschelknautz & Wojahn 1973). This paper initially addresses the improved model for a gas–solids stratified pipe flow from Hong (1992a) and then examines the transition of stratified flow to evaluate the upper and lower boundaries, namely, the theoretical saltation and critical points. Finally, gas–solids stratified flow parameters, solids concentration and velocity, are predicted.

2. BRIEF INTRODUCTION TO THE MODEL FOR GAS–SOLIDS STRATIFIED PIPE FLOW

2.1. Interaction between the suspension and the sliding bed

A key problem in modelling gas–solids stratified flow is the complex interactions between the dilute suspended flow and the dense sliding bed. Four types of particle–particle interaction modes have been ascertained (Hong 1992a, b), that is, saltation, sliding, replacement and insertion of suspended particles over the surface of the sliding bed. The impact of particles at the surface has been roughly analyzed in previous models (Bohnet 1965; Muschelknautz & Krambrock 1969; Wirth & Molerus 1981) and, here, this contribution is given in detail.

Suspended particles collide with the upper part of the pipe wall along with impingement to the surface of the sliding bed. In light of interaction with its boundary, particles in suspension can be divided into: (1) *saltation* over the surface; (2) *sliding* at the surface and (3) *collision* with the pipe wall (figure 1). Different parts of the particles play different roles in the stratified flow and thus, need to be treated respectively. However, in the previous models (Muscheknautz & Krambrock 1969; Wirth & Molerus 1981), all suspended particles were considered to contribute to the shear stress at the surface of the sliding bed only and the additional pressure drop, due to the collision of the part of particles in the suspension with the upper wall, were neglected. Here, we introduce the concept of a particle distribution coefficient to quantify the effects of the different parts of the suspended particles on the flow.

We define the particle distribution coefficients c_1, c_2 and c_3 as the ratios of the number of *saltating*, *sliding* and *colliding* particles to the total number of suspended particles in the dilute suspension, respectively. In the model of Hong *et al.* (1993), c_1 and c_2 have been assumed as a function of the void fraction in the flow

$$c_1 = \left(\frac{\epsilon_1 - \bar{\epsilon}}{\epsilon_1 - \epsilon_2}\right)\left(\frac{\bar{\epsilon} - \epsilon_2}{\epsilon_1 - \epsilon_2}\right) \quad [1]$$

$$c_2 = \frac{\epsilon_1 - \bar{\epsilon}}{\epsilon_1 - \epsilon_2} \quad [2]$$

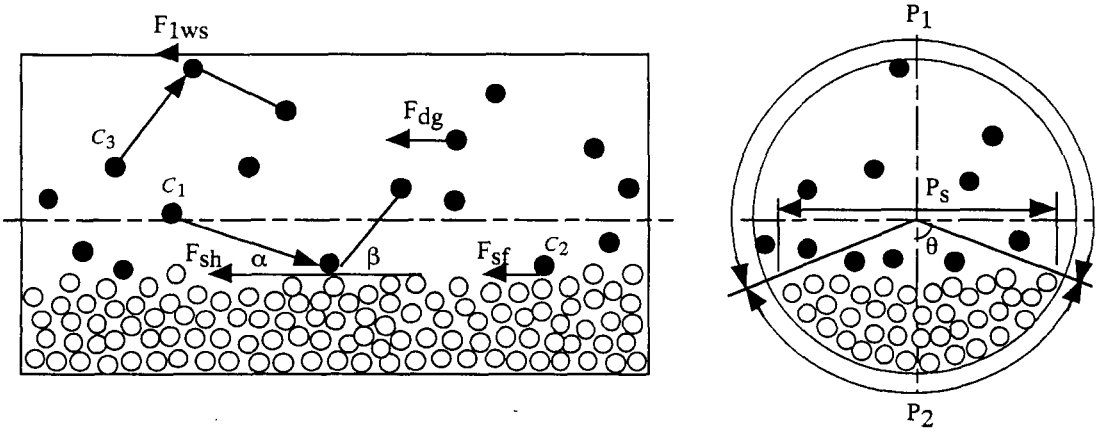

Figure 1. Gas–solids stratified pipe flow.

where ϵ is the void fraction and subscripts 1 and 2 refer to the dilute suspension and dense sliding bed, respectively, and the average void fraction over the cross-section of the pipe $\bar{\epsilon}$ is defined as

$$\bar{\epsilon} = \frac{\epsilon_1 A_1 + \epsilon_2 A_2}{A} \quad [3]$$

where A is the cross-sectional area. The effect of c_3 was simply considered as Yang's solids friction factor (Yang 1974), and this simplification may, however lead to a higher evaluation of the solids friction force (Hong & Shen 1993). For better estimation of solid wall friction due to the collision of suspended particles, c_3 should not be negligible

$$c_3 = 1 - c_1 - c_2 = \left(\frac{\bar{\epsilon} - \epsilon_2}{\epsilon_1 - \epsilon_2}\right)^2 \quad [4]$$

and there are the following relationships between c_1, c_2, c_3 and A_1, A_2 and A

$$\frac{c_1}{c_2} = \frac{A_1}{A} \quad \text{and} \quad \frac{c_1}{c_3} = \frac{A_2}{A_1}$$

We find that [1], [2] and [4] infer the assumptions below:

$$c_1 \leqslant c_2, \quad \text{and} \quad c_3 \leqslant c_1 \text{ if } A_1 \leqslant A_2, \quad \text{and} \quad c_3 \leqslant c_2 \text{ if } A_1 \leqslant 0.5A_2 + \sqrt{0.5(A_2^2 + A_2)}$$

and this means that, compared with saltating over the surface, it is easier for particles to slide along the surface with relatively low energy consumption, and also the particles tend to be saltating at a low gas velocity as the pipe is half filled by the sliding bed.

2.2. Pressure drop for stratified pipe flow

Considering that the shear force exerted by the average gas velocity in the suspension over the surface of the sliding bed is reasonably neglected in this paper since it takes less than 5% of the total forces exerted on the sliding bed and the contribution of c_3 to the solids friction in the upper wall should be included (Hong & Shen 1993), the pressure drop per unit length in the suspension can be rewritten from the model of Hong *et al.* (1993) as

$$\frac{\Delta P}{L} = \frac{f_s c_3 (1-\epsilon_1)\rho_s u_{1s}^2}{2D_1}\frac{P_1}{P_1+P_s} + \frac{\lambda_{1G}\epsilon_1\rho_G u_{1Ga}^2}{2D_1}\frac{P_1}{P_1+P_s} + \frac{c_1(1-\operatorname{tg}\alpha\operatorname{ctg}\beta)\rho_s(1-\epsilon_1)(u_{1s}-u_{2s})u_{1s}P_s}{A_1} + f_{ss}c_2(\rho_s-\rho_G)(1-\epsilon_1)g \quad [5]$$

where ΔP is the pressure drop, L is the pipe length, ρ_s and ρ_G are the solids and gas densities respectively, u_{1s} and u_{2s} are the solids velocity in the suspension and sliding bed, respectively, P_1 and P_s are the wall perimeter of the suspension and width of the surface of the sliding bed, respectively, D_1 is the equivalent diameter of A_1, u_{1Ga} is the actual gas velocity in the suspension, λ_{1G} is the gas friction factor due to the gas phase in the suspension and f_s is the solids friction factor. The impact angle α and lift-off angle β, with the relationships of $\beta = 21.8\alpha^{0.316}$ (White & Schultz 1977), are treated as constant owing to the small variation of α (between 5 and 10° for fine or medium-sized particles). f_{ss} is the internal friction factor and g is the gravitational acceleration.

Similarly, the pressure drop per unit length in the sliding bed can be re-expressed as follows

$$\frac{\Delta P}{L} = f_w\left[\frac{c_2(1-\epsilon_1)(\rho_s-\rho_G)gA_1D\theta}{(1-\epsilon_2)P_sA_2} + \frac{2\operatorname{tg}^2\alpha c_1\rho_s(1-\epsilon_1)u_{1s}^2D\theta}{A_2} + \frac{(1-\epsilon_2)(\rho_s-\rho_G)(\sin\theta-\theta\cos\theta)gD^2}{2A_2}\right] + \frac{\lambda_{2G}\epsilon_2\rho_G u_{2Ga}^2}{2D_2}\frac{P_2}{P_2+P_s} - \frac{(1-\operatorname{tg}\alpha\operatorname{ctg}\beta)c_1\rho_s(1-\epsilon_1)(u_{1s}-u_{2s})u_{1s}P_s}{A_2} - \frac{f_{ss}c_2(\rho_s-\rho_G)(1-\epsilon_1)gA_1}{A_2} \quad [6]$$

in which f_w is the wall friction factor, D is the pipe diameter, θ the angle defined in figure 1, P_2 the wall perimeter of the sliding bed, D_2 the equivalent diameter of A_2, λ_{2G} the gas friction factor due to the gas phase in the sliding bed and u_{2Ga} the actual gas velocity in the sliding bed.

Therefore, the pressure drop per unit length in stratified flow should be as below

$$\frac{\Delta P}{L}=\frac{f_w A_2}{A}\left[\frac{c_2(1-\epsilon_1)(\rho_s-\rho_G)gA_1D\theta}{(1-\epsilon_2)P_sA_2}+\frac{2\,\mathrm{tg}^2\,\alpha c_1\rho_s(1-\epsilon_1)u_{1s}^2D\theta}{A_2}\right.$$
$$\left.+\frac{(1+\epsilon_2)(\rho_s-\rho_G)(\sin\theta-\theta\cos\theta)gD^2}{2A_2}\right]+\frac{\lambda_{2G}\epsilon_2\rho_G u_{2Ga}^2}{2D_2}\frac{P_2}{P_2+P_s}\frac{A_2}{A}$$
$$+\frac{f_s c_3(1-\epsilon_1)\rho_s u_{1s}^2}{2D_1}\frac{P_1}{P_1+P_s}\frac{A_1}{A}+\frac{\lambda_{1G}\epsilon_1\rho_G u_{1Ga}^2}{2D_1}\frac{P_1}{P_1+P_s}\frac{A_1}{A} \qquad [7]$$

2.3. Mass balance for stratified flow

The mass balance for solids and the gas phase in stratified flow is respectively given as

$$M_s=M_{1s}+M_{2s} \qquad [8a]$$

or

$$\rho_s(1-\bar{\epsilon})u_sA=\rho_s(1-\epsilon_1)u_{1s}A_1+\rho_s(1-\epsilon_2)u_{2s}A_2 \qquad [8b]$$

and

$$M_G=M_{1G}+M_{2G} \qquad [9a]$$

or

$$\rho_G\bar{\epsilon}u_{Ga}A=\rho_G\epsilon_1u_{1Ga}A_1+\rho_G\epsilon_2u_{2Ga}A_2 \qquad [9b]$$

where M_s, M_{1s} and M_{2s} are the mass flowrates of the solids in stratified flow, the suspension and the sliding bed, respectively, and M_G, M_{1G}, M_{2G} represent the mass flowrates of the gas phase in stratified flow, the suspension and the sliding bed, respectively, u_s and u_{Ga} are the average solids velocity and actual gas velocity, respectively.

2.4. Calculation approach and conditions

An approach has been developed based on the trial and error method of Hong *et al.* (1993), as shown in figure 2, to analyze the upper and lower boundaries of the gas–solids stratified pipe flow based on the widely used assumptions that $u_{2s}=u_{2Ga}$ and the void fraction in the sliding bed, ϵ_2, equals that of a loosely packed bed ϵ_b. The calculation proceeds as follows:

(1) the properties of the solids ρ_s, ρ_G, ϵ_b, d_s (particle diameter), f_{ss}, f_w and the operating parameters M_s, M_G, D are given as initial values;

(2) an initial value is given to ϵ_1;

(3) a value for θ is assumed to calculate the geometric conditions P_1, P_s, A_1, A_2, D_1, D_2, the height of the sliding bed

$$H_b=0.5D(1-\cos\theta) \qquad [10]$$

and the suspended particle distribution coefficients c_1, c_2, c_3;

(4) Calculate u_{1Ga}, u_{1s}, the solids mass flow rate in suspension M_{1s} and if $M_{1s}\leqslant 0$, return to step (3) with a new increased value of θ and if $H_b\leqslant D$ at the largest $\theta_{max}=\pi-\arccos(1-2d_s/D)$, restart from step (2) with a newly decreased ϵ_1 and if $H_b\leqslant D$ for $\epsilon_1=\epsilon_b$ at the largest $\theta_{max}=\pi-\arccos(1-2d_s/D)$ is not satisfied, then the flow for the material and operating parameters must be a dense plug flow;

(5) calculate M_{2s}, u_{2s} and the particle relative velocity $U_1=u_{1s}-u_{2s}$ and if $M_{2s}\leqslant 0$, go back to step (3) with a new decreased value of θ and then if $H_b\leqslant d_s$ at the smallest $\theta_{min}=\arccos(1-2d_s/D)$, return to step (2) with a new decreased ϵ_1 and finally if $H_b\geqslant d_s$ at $\epsilon_1=\bar{\epsilon}$ is not satisfied, then the flow for the initial values in step (1) must be a dilute suspended flow and the corresponding gas velocity should be termed as the theoretical saltation velocity;

(6) predict the pressure drop in the suspension and sliding bed using [5] and [6] and, if the former is smaller than the latter, return to step (3) by choosing a new decreased θ until the two predicted pressure drops agree within the prescribed error; otherwise a new increased θ is used in step (3);

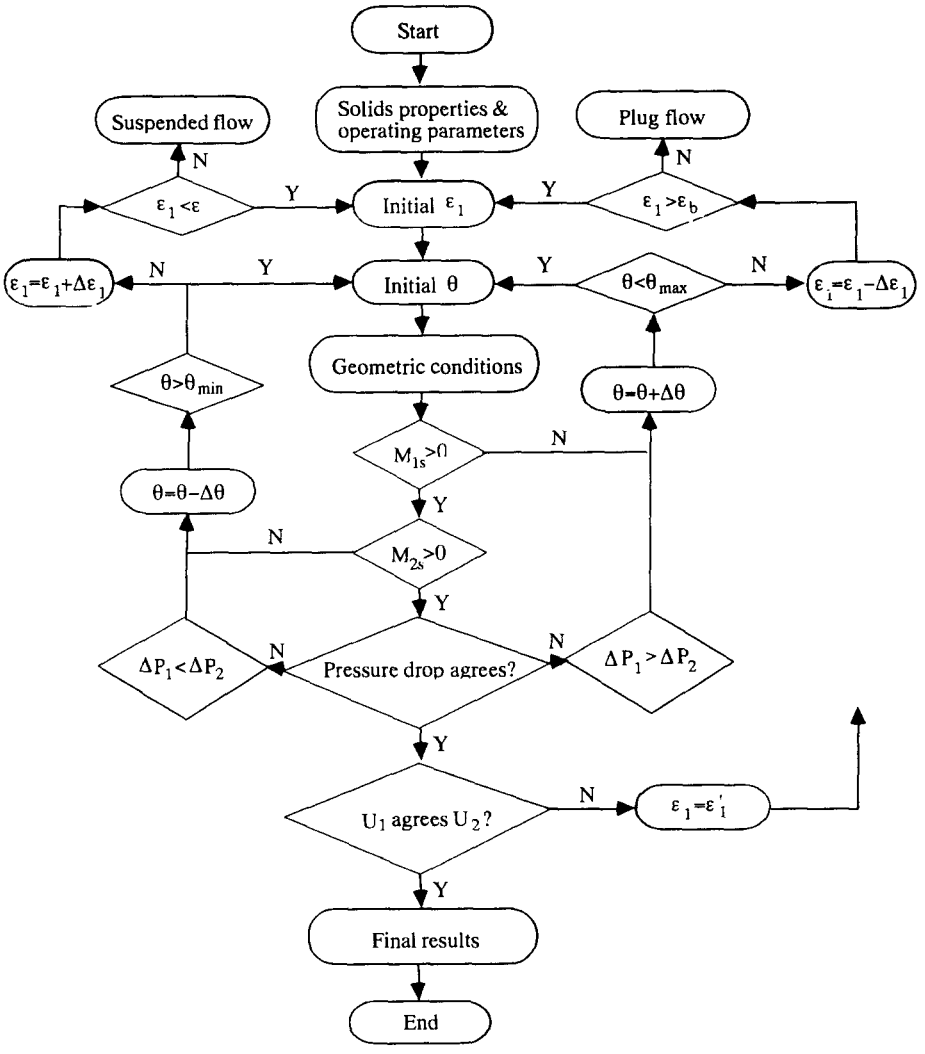

Figure 2. Flow diagram of gas–solids stratified pipe flow predictive model.

(7) recalculating the relative particle velocity $U_2 = u_{1s} - u_{2s}$ included in the term of shear force per volume of suspension, F_{sh}, caused by the impact of saltating particles upon the sliding bed with the following force equation for suspended particles:

$$(1-\epsilon_1)\frac{\Delta P}{L} = F_{1ws} + F_{sh} + F_{sf} + F_{dG} \qquad [11]$$

where F_{1ws} refers to the wall friction forces averaged over the total volume of the suspension due to the solids in suspension and expressed as a form similar to the Fanning equation (Yang 1974; Klinzing *et al.* 1987)

$$F_{1ws} = \frac{f_s c_3 (1-\epsilon_1)\rho_s u_{1s}^2}{2D_1}\frac{P_1}{P_1+P_s}, \qquad [12]$$

F_{sh} is the shear force averaged over the total volume of suspension:

$$F_{sh} = \frac{c_1(1-\operatorname{tg}\alpha\operatorname{ctg}\beta)\rho_s(1-\epsilon_1)(u_{1s}-u_{2s})u_{1s}P_s}{A_1} \qquad [13]$$

and F_{sf} is the friction force attributable to the sliding particles averaged over the total volume of the suspension:

$$F_{sf} = f_{ss} c_2 (\rho_s - \rho_G)(1-\epsilon_1)g \qquad [14]$$

while F_{dG} is the gas drag force due to the gas phase in the suspension averaged over the total volume of the suspension. The correlation of Arastoopour & Gidaspow (1979) valid for a dense suspension is adopted here

$$F_{dG} = \frac{3C_d\epsilon_l^{-2.65}(1-\epsilon_l)(u_{lGa}-u_{ls})^2\rho_G}{4d_s} \quad [15a]$$

with the drag coefficient C_d

$$C_d = \frac{24(1+\mathrm{Re}_d^{0.687})}{\mathrm{Re}_d} \quad \text{for } \mathrm{Re}_d < 10^3 \quad [15b]$$

$$C_d = 0.44 \quad \text{for } \mathrm{Re}_d > 10^3 \quad [15c]$$

where

$$\mathrm{Re}_d = \frac{\epsilon_l|u_{lGa}-u_{ls}|d_s\rho_G}{\mu_G} \quad [15d]$$

and if U_2 is approximate to U_1 within the prescribed error, then

(8) the results can be output, otherwise the assumed value of ϵ_l in step (2) should be replaced by a new one modified by U_2

$$\epsilon_l' = 1 - \frac{M_{ls}}{A_1\rho_s\left[\dfrac{M_{2s}}{(1-\epsilon_b)A_2\rho_s} + U_2\right]} \quad [16]$$

With the above procedure, gas–solids stratified pipe flow can be analyzed. It should be pointed out that the computation is quite sensitive to the initial values of ϵ_l and θ as well as their increments. The choice of these initial values is strongly dependent on material properties and operating parameters. In the present analysis, initial $\epsilon_l = 0.99$, $\theta = \pi/3$ and increments $\Delta\epsilon_l = 0.001$, $\Delta\theta = 2\pi \times 10^{-6}$ are chosen for the relative error of the final calculation results $\delta < 1\%$.

2.5. Comparison between the model of Hong et al. and the present improved model

The model of Hong *et al.* was compared with experiments for medium-sized sand and fine lime particles conveyed in a 20 mm pipe in figure 3 of Hong *et al.* (1993). As a comparison to the model of Hong *et al.*, figures 3(a) and (b) also represent these $(\Delta P/L)$–u_G phase-diagrams (u_G superficial gas velocity) with solids loading m^* as a parameter for medium-sized sand and fine lime particles, respectively, from both the previous model of Hong *et al.* and the present improved model. Different from the assumption for the impact angle $\alpha = 7.5°$ for both medium-sized sand and fine lime in the model of Hong *et al.*, according to the descriptions for saltation in section 1, it is more reasonable to separately assume the impact angle $\alpha = 10°$ for medium-sized sand and $\alpha = 7.5°$ for fine lime in the prediction of the improved model. As shown, even though the higher impact angle assumed to medium-sized sand leads to a greater pressure drop, the present improved model predicts a much better phase diagram (particularly for medium-sized sand) compared with the experimental data than the previous model of Hong *et al.* This may be attributed to the fact that the higher the solids loading, the more remarkable the difference between the previous and present models, especially at a relatively larger superficial gas velocity.

In the following sections, predictions are made from the present improved model for fine lime particles with the calculation condition shown in table 1, and the predictive results are presented with the solids mass flowrate parameter since many published experimental results were obtained with this parameter as constant.

3. ANALYSIS OF TRANSITION OF FLOW REGIMES

3.1. Saltation velocity: transition between suspension and stratified flow

A widely used definition for saltation velocity has been given as the superficial gas velocity where the minimum pressure-drop occurs in the phase diagram. The Rizk's correlation (1976) gives the minima in the phase diagram with solids flowrate as a parameter by:

$$\frac{M_s}{M_G} = \frac{(\mathrm{Fr}_{sa})^{1.1d_s+2.5}}{10^{1.44d_s+1.96}} \quad [17]$$

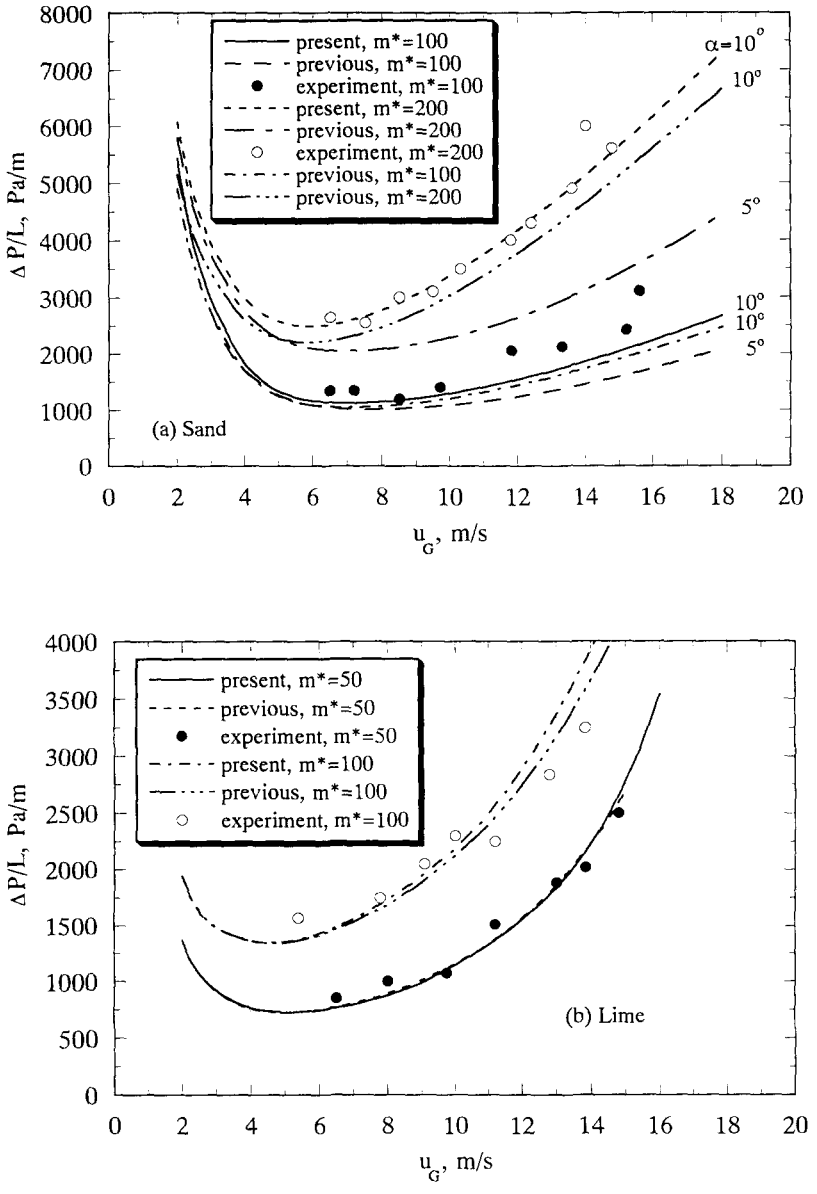

Figure 3. Comparison between phase diagrams from the previous model of Hong *et al.* and the present improved model.

where Fr_{sa} is the saltation Froude number ($u_{sa}/\sqrt{gD}$) and d_s in millimetres. Many investigators recognized that the experimental minimum point in the phase diagram coincides with the occurrence of saltation phenomenon, that is, the particles are observed to drop out of suspension and then, travel along the pipe by rolling or sliding or remain in a stationary bed on the bottom of the pipe dependent on the particles. Different from the experimental determination of saltation point in the phase diagram which is usually full of the researcher's subjectivity, in this paper, a theoretical saltation point is directly defined as the superficial gas velocity where the height of sliding bed equals to particle diameter, $H_b = d_s$, as the upper boundary of stratified flow (also the lower limit of suspension flow) based on the original meaning of saltation.

The calculated relationship between dimensionless height of sliding bed H_b/D and Froude number ($Fr = u_G/\sqrt{gD}$) is presented in figure 4. The theoretical saltation point is almost the intersection with the abscissa owing to $d_s \ll D$. For a given M_s, the increase of Fr at theoretical saltation point with reducing D is associated with the increase of solids concentration, and

Table 1. Calculation conditions

Material—lime	
Density (kg/m^3)	3250
Diameter (mm)	0.083
Terminal velocity of single particle (m/s)	0.66
Internal friction coefficient (-)	0.74
Voidage of loosely packed bed (-)	0.76
Wall friction factor* (-)	0.58
Operating parameter	
Solids mass flowrate (kg/s)	1.0, 1.5
Pipe diameter (mm)	40, 60, 80, 100
Air density (20C°) (kg/m^3)	1.21
Impact angle (°)	7.5

†Measured in steel pipe.

theoretical saltation velocity decreases as the pipe size grows since the larger the pipe, the smaller the dispersed density. Consequently, the particles separate out of gas–solids suspension at a lower velocity, and the effect of D on theoretical saltation point is becoming less significant at larger pipes due to the smaller variation of solids concentration with the pipe diameter (see figure 7). Moreover, numerical calculations show that turning points (or inflexion point) exist in this figure.

The difference between Rizk's correlation and present theoretical saltation Fr_{sa} is partially attributable to the coarser particles used in Rizk's correlation. Figure 4 shows that for larger pipes, the theoretical saltation points tend towards Rizk's ones, whereas the extension of Rizk's correlation might be unreasonable at much smaller pipes or high density flow. Since the Rizk saltation points are based on the experiments conducted at non-transparent pipes and are actually minima in phase diagram, they should be different from theoretical saltation points. That is, particles drop out of gas phase at a velocity higher than Rizk's point, in particular in smaller pipes or high density flow, and Rizk's point seems to be superficial instead of the real saltation point. One reason why Rizk's correlation is strongly recommended may be reached through the variation of H_b with Fr. Once the particle begins to drop out of suspension at the theoretical saltation point, a small decrease of gas velocity causes a rapid increase of H_b until the turning point and this point is quite close to Rizk's point. It seems difficult to observe the occurrence of the particle layer of

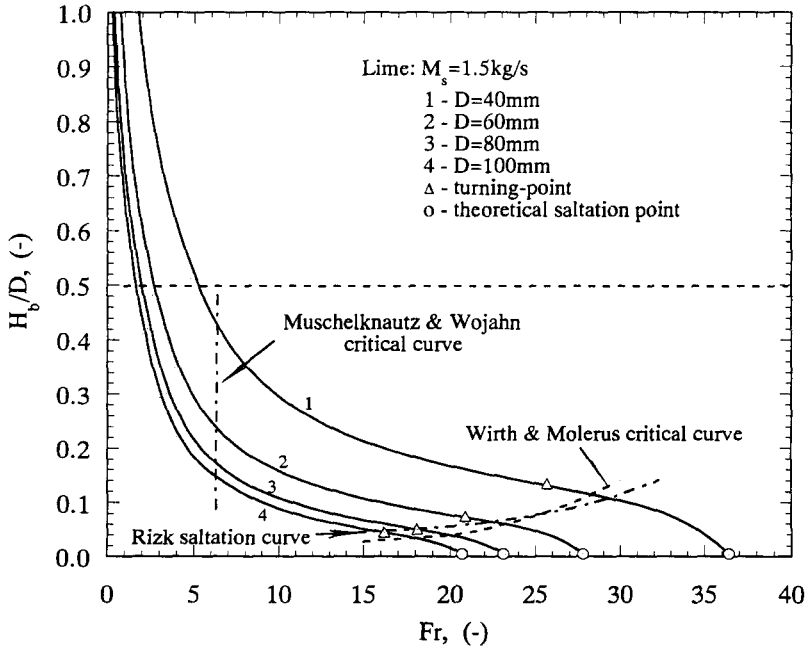

Figure 4. Variation of dimensionless height of the sliding bed with Froude number.

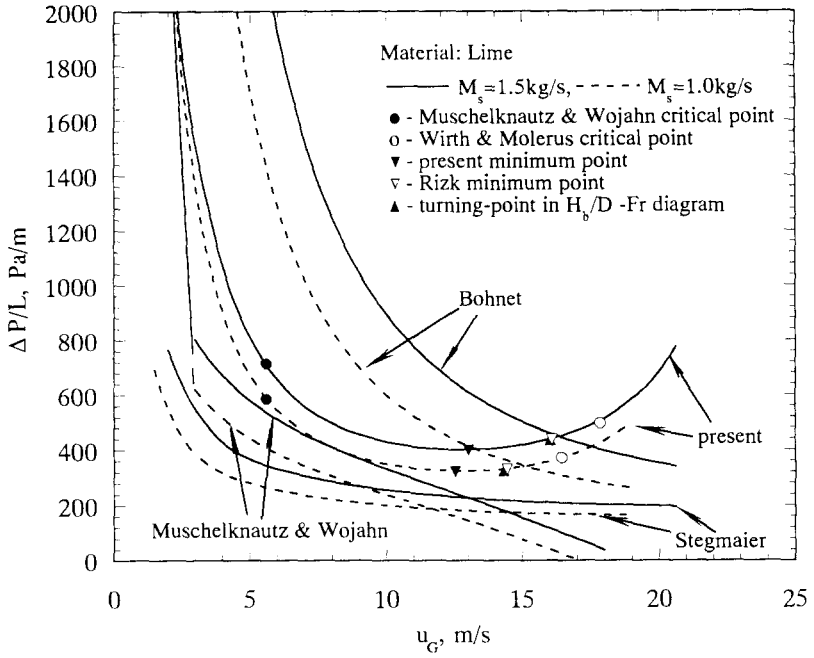

Figure 5. Predictive phase diagram from different models.

one particle diameter height, especially for fine powders. Consequently, it is possible that Rizk's point is corresponding to the particle layer of many times the particle diameter which is easily observable.

Figure 5 shows the pressure drop-velocity phase diagram by the models of Bohnet (1965), Muschelknautz & Wojahn (1973), Stegmaier (1978) and the present improved model. The other three models, except the present one, show non-minimum and monotonously decreasing curves. The present model suggests a flat curve in the vicinity of the pressure drop minima which is similar to the experiments performed by Wirth & Molerus (1986) for lower solids flowrate, and in general, the turning point determined in the diagram of H_b/D versus Fr is close to the Rizk's point. The gas velocity at the present pressure drop minimum point is lower than Rizk's ones. This may be explained by the fact that, around the minimum point, the predicted curve is so flat that the present minimum pressure drop tends to that at Rizk's point. Furthermore, the pressure drop to the right of Rizk's point quickly increases with gas velocity and this possibly results in incorrect choosing of Rizk's point as the real minimum pressure drop point since it seems rather difficult to discriminate the real minimum from the measured pressure drop curves. Meanwhile, the gas velocity at minimum point is found to increase with M_s as confirmed by many researchers (Zenz & Othmer 1960; Wirth & Molerus 1986).

In summary, the present model shows that the saltation point may be different from the minimum pressure drop point in the phase diagram. Rizk's point seems to be the turning point determined in H_b/D versus Fr diagram which is located just between the real minimum pressure drop and real saltation points. That is, particle begins to separate from the gas phase at a velocity greater than that at both Rizk's "saltation" point and real minimum pressure drop point. However, it is recognized that the more dilute the gas–solids flow, the closer the three points and this indicates the validity of Rizk's correlation in dilute pneumatic transport.

3.2. Critical velocity: transition between stratified flow and unstable plug flow

Critical velocity is the minimum conveying velocity avoiding the blockage of the pipe. Therefore, the critical point could be theoretically defined at $H_b/D = 1$. An increase in Fr from this theoretical point until the turning point existing in the H_b/D versus Fr diagram leads to a sharp decrease of H_b, and the flow is very sensitive to the small variation of gas and solids supply. Furthermore, the pressure drop strongly changes and hence, a stable stratified flow cannot be realized at $H_b/D = 1$.

Therefore, from the viewpoint of stability and safety, Muschelknautz & Wojahn (1973), Wirth (1983) and Wirth & Molerus (1986), defined the critical velocity as the transition between the temporally constant pressure drop behavior of stratified flow and the strongly fluctuating pressure drop of plug flow, namely, the minimum gas velocity required for the stable stratified flow. For fine particles, Muschelknautz & Wojahn (1973) suggested that the critical Froude number Fr_{cr} is independent of M_s

$$Fr_{cr} = \frac{u_{cr}}{\sqrt{gD}} \approx 0.25\sqrt{\frac{\rho_{sb}}{\rho_G}} \quad \text{for } \frac{M_s}{M_g}\frac{\rho_G}{\rho_{sb}} < 0.75 \qquad [18]$$

where ρ_{sb} is the density of sliding bed and here taken as $(1-\epsilon_b)\rho_s$. On the other hand, a dimensionless equation of Wirth & Molerus (1981, 1986) gives critical velocity u_{cr} to be independent of D for a given M_s in a wide range of particle

$$\frac{\rho_G}{\rho_s(1-\epsilon_b)}\frac{M_s}{M_G} = 0.018\left[\frac{Fr_{cr}}{\sqrt{\left(\frac{\rho_s}{\rho_G}-1\right)(1-\epsilon_b)f_w}}\right]^4 \qquad [19]$$

In figure 4, Muschelknautz & Wojahn's critical point lies in the section where H_b/D sharply increases, and is between the present theoretical critical point and turning point. It is noted that, as D increases, the turning point tends towards Muschelknautz & Wojahn's critical point. Figure 6 shows the dimensionless suspension cross-sectional area by the present and Muschelknautz & Wojahn models, and the theoretical critical point is at $A_1/A = 0$, while the theoretical saltation point is at the position near $A_1/A = 1$. The present model agrees well with the Muschelknautz & Wojahn model. This means that the gas velocity at Muschelknautz & Wojahn's point seems reasonable as critical velocity for the purpose of safety although it somewhat arbitrarily keeps constant in figures 4 and 6.

Obviously, the gas velocity at Muschelknautz & Wojahn's critical point is lower than that at the "saltation" point which refers minimum pressure drop point as described by Wirth & Molerus (1986). Wirth & Molerus critical point has been found to be far from Muschelknautz & Wojahn's critical point, almost overlaps both Rizk's saltation point and the turning point when the pipe increases as shown in figure 4. That is, Wirth & Molerus's critical point is more similar to the turning point than Muschelknautz & Wojahn's critical point expecially in the case of smaller

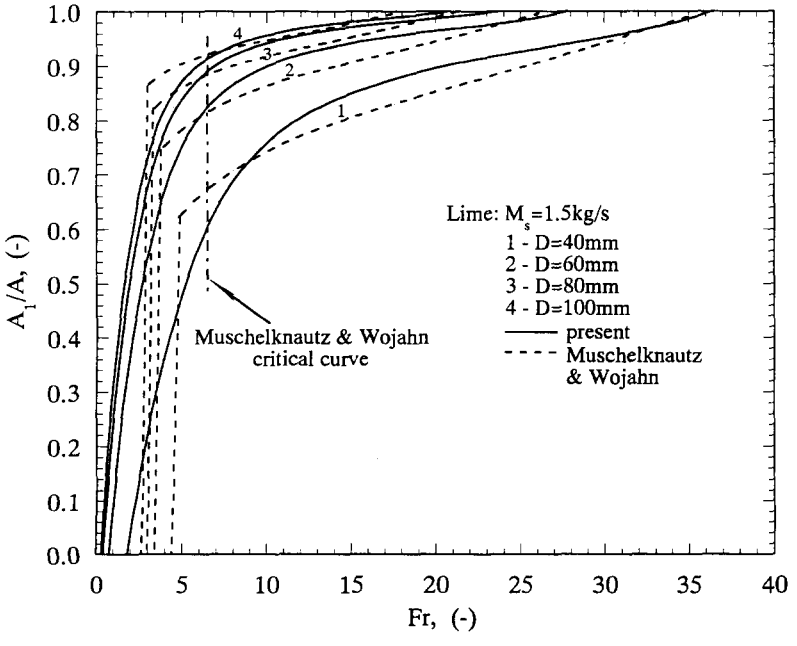

Figure 6. Dimensionless suspension area A_1/A vs Froude number.

pipes while the present model agrees with Muschelknautz & Wojahn results. No matter which critical point is concerned, the height of the sliding bed for stable stratified flow is found to rarely exceed half the pipe diameter.

As a whole, this model suggests that the present theoretical critical point is of impractical use for designers in most cases, although they provide the minimum velocities for given flow conditions, since they are already located at very low Fr corresponding in general to high flow pressure drop and its strong fluctuation. Muschelknautz & Wojahn critical velocity seems more reasonable, whereas Wirth & Molerus critical velocity appears too high for high density transport of fine particles and is close to the turning point. Moreover, it is found that as the gas–solids flow turns more and more dilute or say solids concentration turns smaller (see section 4.1), all the points mentioned above become closer and closer, and the range of stratified flow becomes narrow. This implies that it is more difficult to perform a stable stratified flow at a relatively more dilute flow condition, for example, at larger pipes for a given solids flowrate or at smaller solids flowrate for a given pipe.

4. SOLIDS CONCENTRATION AND VELOCITY IN HIGH DENSITY STRATIFIED FLOW

4.1. Variation of solids concentration

Solids concentration varies with the operating parameters. Plot of average solids volumetric concentration C_s (i.e. $1-\bar{\varepsilon}$) in stratified flow against Froude number at different mass flowrates is given in figure 7. The theoretical saltation line divides the stratified flow from suspended flow, and indicates the minimum solids concentration in stratified flow and the maximum capacity of suspendingly conveying solids. It is found that, generally, the maximum solids concentration in suspension decreases with increase in pipe size or reduction of solids flowrate. This shows that there are at least two approaches to accomplish high density suspension: decreasing pipe size and increasing solids flowrate. Because suspended flow occupies the region of quite low solids concentration, unless special measure is taken, it seems almost impossible in industry to reach fully suspended high density flow with $C_s > 0.05$ owing to the practice of wing larger pipes ($D > 80$ mm) even if different materials are employed.

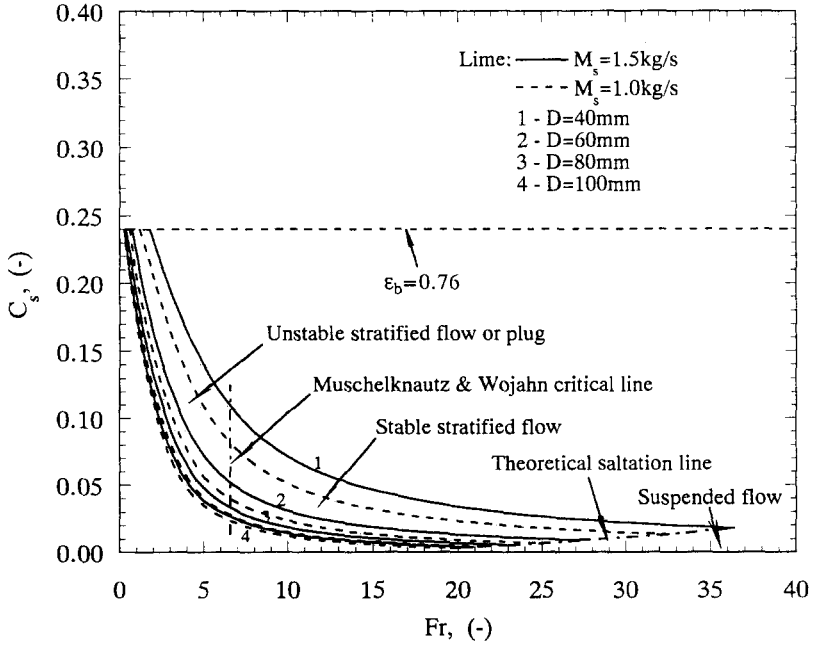

Figure 7. Average solids volumetric concentration vs Froude number.

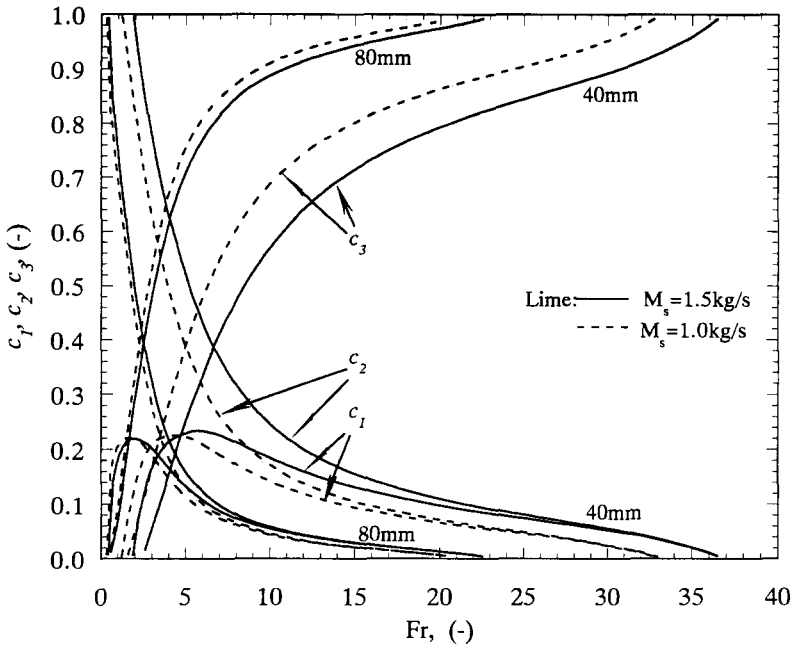

Figure 8. Suspended particle distribution coefficient vs Froude number.

In stratified flow, reduction in Fr generates increase of C_s until its maximum $1 - \epsilon_b$ where the pipe is fully filled with solids particles. The Muschelknautz & Wojahn critical line might be the division between stable and unstable stratified flow or plug flow. As shown, the stable stratified flow exists at a rather lower C_s than its loosely packed concentration $1 - \epsilon_b$. Apparently, the variation of C_s is somewhat similar to that of the height of the sliding bed. This simply implies that at larger Fr, C_s is mainly influenced by the suspension layer, whereas at low Fr, the sliding bed determines C_s. Both suspension and sliding bed contribute to C_s at a moderate Fr which corresponds to a field of stable stratified flow.

In the stable stratified flow, the increment of C_s for a given M_s is inversely proportional to D. For a fixed pipe, the difference of C_s among different M_s becomes smaller as Fr grows. In other words, the larger the pipe, the smaller the effects of Fr and M_s on C_s. This confirms that, in large pipes, a high density flow is obtainable only in an unstable stratified or plug flow at low Fr irrespective of M_s while, in small pipes, stable stratified flow is easily strengthened in a high density with the increase of M_s irrespective of Fr.

4.2. Distribution of suspended particles

Since the suspended particle distribution coefficients c_1, c_2 and c_3 are defined based on the average void fraction over the area, they are independent of material, solids mass flowrate and pipe size for a fixed H_b/D. Figure 8 depicts the relationship between c_1, c_2, c_3 and Froude number Fr. At first glance, the curves of c_2 resemble that for the height of the sliding bed. With the increase of bed height, the number of particles c_3 colliding with the upper wall decreases and the suspended particles tend to concentrate over the surface. Furthermore, c_3 is higher than c_1 and c_2 at larger Fr, and c_1 is low throughout and becomes lower as the bed develops, i.e. most suspended particles usually belong to those sliding rather than saltating especially at lower Fr. In detail, in $H_b/D < 0.5$, the ratio of saltating particle c_1 is the smallest and increases with the bed until its maximum value 0.25, and in $H_b/D > 0.5$, c_1 will be greater than c_3 but both c_1 and c_3 reduce sharply with Fr. This means, throughout stratified flow, the saltating particles are assumed to take a small part, 25 percent at most, of suspended particles although they are thought to play the most important role in the movement of sliding bed (Muschelknautz & Krambrock 1969; Wirth & Molerus 1981; Hong & Shen 1993). It is predictable that a higher evaluation of c_1 leads to the increase in the shear force over the surface from the impingement of the saltating particle and thus the sliding bed will

disappear at a lower Fr, or the theoretical saltation point will be smaller than the present one. The distribution of suspended particles is brought from a supposition based on the facts at two extreme cases of flow. Nevertheless, this distribution provides a way of allowing for the evaluation of the different interactions between the suspension and the sliding bed.

4.3. Solids velocity

Figure 9 depicts the velocity ratio of solids to actual gas u_s/u_{Ga}. For a given pipe and M_s, the ratio initially decreases with the decrease of Fr and then, at a certain Fr, the ratio increases steeply. This is due to the fact that the greater the Fr, the smaller the C_s, i.e. the stratified flow becomes much more dilute, the higher the ratio of u_s/u_{Ga}. On the other hand, at lower Fr, the sliding bed is usually dominant and develops sharply with reducing Fr. Consequently, it is natural that the ratio u_s/u_{Ga} grows due to the assumption of $u_{2s} = u_{2Ga}$. The steeper curve in larger pipes can be explained as the narrow range of existence of stratified flow. Obviously, there exists a significant difference between the prediction and the simple experimental correlation, $u_s/u_{Ga} = 0.5$, obtained at high density flow (solids loading 80–750) by Wen & Simons (1959).

Figure 10 compares the predicted ratio of velocity of the sliding bed to superficial gas velocity u_{2s}/u_G from Bohnet (1965), Muschelknautz & Wojahn (1973) and the present models. As shown, there is considerable difference between these models. Bohnet's model neglects the particle–particle interaction between suspension and sliding bed, and is independent of materials, pipe size and solids flowrate. On the contrary, the Muschelknautz & Wojahn model predicts that the ratio decreases with increasing Fr and for a given solids flowrate, the greater the pipe, the smaller the ratio. However, the present model shows that at larger Fr, the ratio u_{2s}/u_G increases with Fr due to the increase of shear driving-force from the suspended particles of higher velocity and the decrease of friction resistance at lower pipe wall whereas, at lower Fr, an inverse trend happens to this ratio resulting from the sharp increase of resistance of the sliding bed corresponding to the steep increase of its height. The model of Muschelknautz & Wojahn seems to be invalid at higher Fr since it leads to naught or negative pressure drop finally (the negative section of curve of the Muschelknautz & Wojahn model has not been depicted in figure 5). In fact, the figures show that the higher the solids concentration, the closer the calculations between Muschelknautz & Wojahn and present models and contrarily, the lower the solids concentration, the closer the predictions between Bohnet and present models. This coincides with the conclusions of Bohnet (1990) that this model cannot predict pressure drop well if solids loading exceeds 20–50.

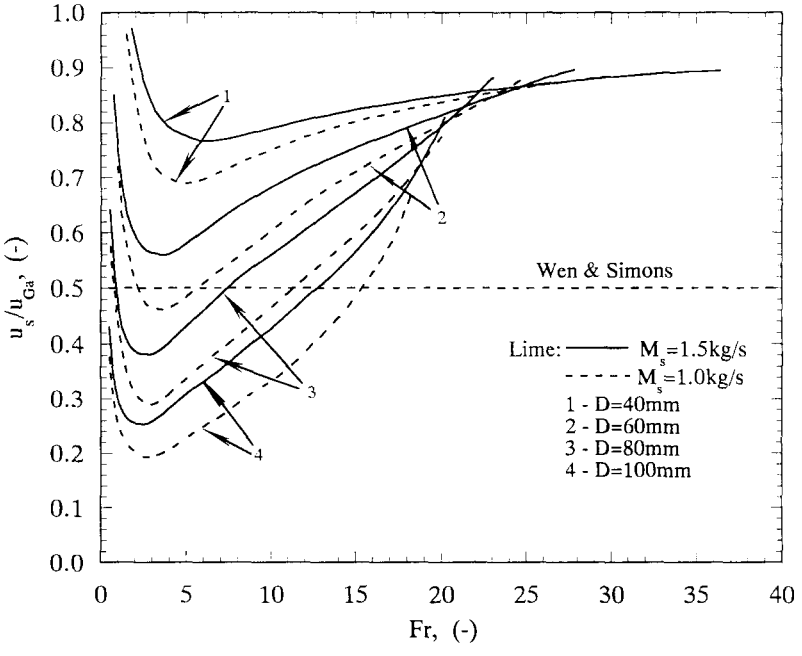

Figure 9. Velocity ratio of solids to actual gas vs Froude number.

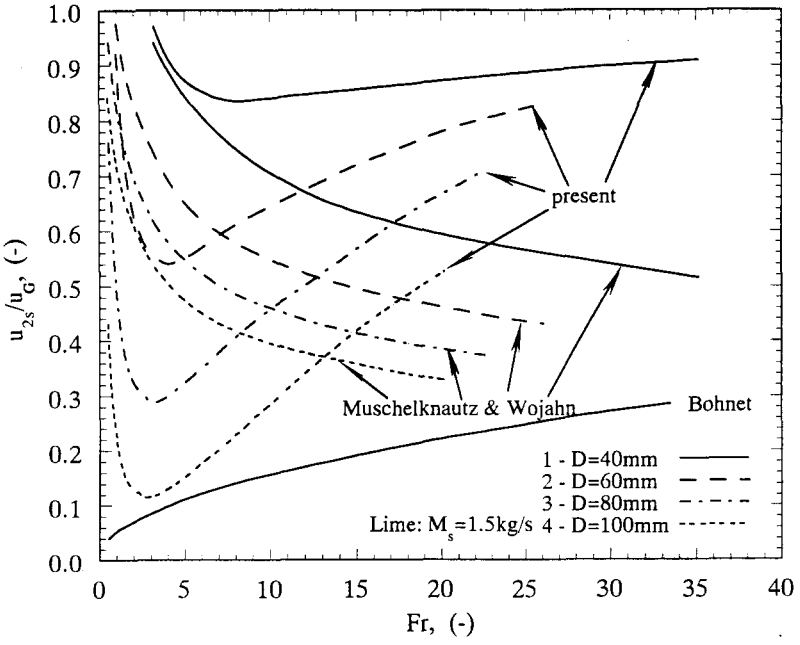

Figure 10. Velocity ratio of sliding bed to superficial gas vs Froude number.

The same effects of pipe size and solids flowrate on the ratio of u_{2s}/u_G have been predicted by Muschelknautz & Wojahn and this model. Increase in the pipe diameter causes the ratio u_{2s}/u_G to decrease at a fixed solids flowrate while the ratio increases with solids flowrate at a given pipe. However, it should be pointed out that, in the Muschelknautz & Wojahn model, the ratio of u_{2s}/u_G is actually independent of solids loading for a specific material.

5. CONCLUDING REMARKS

An improved model, which accounts for the interactions between a dilute suspension and a dense sliding bed in gas–solids stratified pipe flow, has been briefly presented to predict the transition of gas–solids stratified flow. The turning point determined in the diagram of the dimensionless height of the sliding bed versus Froude number is found to be close to Rizk's saltation point. The present model shows that the particles begin to drop out of gas phase at a theoretical saltation point at which the velocity is greater than that at Rizk's saltation point and a higher evaluation of the number ratio of saltating particles than that in the present model will result in a smaller theoretical saltation velocity. Muschelknautz & Wojahn's critical point seems valid for a stable stratified flow of fine particles. However, as the flow becomes dilute, the turning point tends to be much closer to Rizk's point, and the difference between the saltation point of the present model and Rizk's correlation and the critical point by Muschelknautz & Wojahn and Wirth & Molerus becomes smaller. This leads to the relative difficulty of performing stable stratified flow in larger pipes or a smaller solids flowrate in practice.

The stable gas–solids stratified flow exists at a rather lower average solids concentration than that of its loosely packed bed. The present predictions for solids velocity indicate that, the velocity ratios of solids-to-actual gas and sliding bed-to-superficial gas increase with Froude number, except for the lower Froude number due to the assumption that the solids velocity in a sliding bed is equal to the actual gas velocity. Furthermore, an assumed distribution of suspended particles shows that only a small part of the suspended particles saltate over the surface although they play a decisive role in the interaction between the suspension and the sliding bed of the stratified flow, and this distribution needs to be verified in experiments.

Acknowledgement—One of the authors (J. Hong) wishes to thank the Japanese Ministry of Science, Culture and Education for their Research Scholarship for this work.

REFERENCES

Arastoopour, H. & Gidaspow, D. 1979 Vertical pneumatic conveying using four hydrodynamic models. *I & EC Fund.* **18,** 123–130.

Bagnold, R. A. 1941 *The Physics of Blown Sand and Desert Dunes.* Methuen, London.

Bohnet, M. 1965 Experimentelle und theoretische Untersuchungen uber das Absetzen, das Aufwirbeln und den Transport feiner Staubteilchen in pneumatischen Förderleitungen. *VDI-Forschungsheft* **507.**

Bohnet, M. 1985 Advances in the design of pneumatic conveyors. *Int. Chem. Engng* **25,** 386–405.

Bohnet, M. W. 1990 Dense-phase pneumatic conveying. In *Proc. of Second World Congress on Particle Technology, Part II: Storage and Conveying*, Kyoto, Japan, pp. 84–91.

Chepil, W. S. 1945 Dynamics of wind erosion: I. The nature of movement of soil by wind. *Soil Sci.* **60,** 305–320.

Doig, I. D. 1975 Design and performance aspects of dense phase pneumatic conveying systems. *Sth Afri. Mech. Engng* **25,** 394–403.

Geldart, D. & Ling, S. J. 1992 Saltation velocity in high pressure conveying of fine coal. *Powder Technol.* **69,** 157–162.

Hong, J. 1992a Horizontal medium phase pneumatic conveying of fine and medium particles. Ph.D. thesis, University of Science & Technology, Beijing, PRC.

Hong, J. 1992b Behaviors of particles in gas-solid two-phase stratified flow. Presented at the *20th Int. Congress on High Speed Photography and Photonics*, Victoria, B.C., Canada.

Hong, J. & Shen, Y. 1993 Mechanism of high density gas-solids transport in horizontal pipes. In *Proc. 4th National Conf. on Multiphase Fluid, Non-Newtonian Fluid and Physicochemical Fluid Flows*, Xi'an, PRC, pp. 56–62.

Hong, J., Shen, Y. & Liu, S. 1993 A model for gas–solids stratified flow in horizontal dense-phase pneumatic conveying. *Powder Technol.* **77,** 107–114.

Jones, P. J. & Leung, L. S. 1978 Estimation of saltation velocity in horizontal pneumatic conveying—a comparison of published correlation. In *Proc. of Pneumotransport 4*, Bedford, U.K., paper C1, pp. 1–12.

Klinzing, G. E., Rohatgi, N. D., Zaltash, A. & Myler, C. A. 1987 Pneumatic transport—a review (generalized phase diagram approach to pneumatic transport). *Powder Technol.* **51,** 135–149.

Konrad, K. 1986 Dense-phase pneumatic conveying: a review. *Powder Technol.* **49,** 1–35.

Lucht, T. R. & Soo, S. L. 1990 Density and its fluctuation in stratified flow of a dense particulate suspension. In *Proc. of Second World Congress Particle Technology, Part II: Conveying and Storage*, Kyoto, Japan, pp. 53–60.

Marcus, R. D., Leung, L. S., Klinzing, G. E. & Rizk, F. 1990 *Pneumatic Conveying of Solids.* Chapman & Hall, London.

Molerus, O. & Wirth, K.-E. 1991 State diagrams of gas/solid flows with partial phase separation. *KONA-Powder Sci. Technol. Jap.* **9,** 159–173.

Muschelknautz, E. & Krambrock, W. 1969 Vereinfachte Berechnung horizontaler pneumatischer Förderleitungen bei höher Gutbeladung mit feinkörningen Produkten. *Chem.-Ing.-Tech.* **41,** 1164–1172.

Muschelknautz, E. & Wojahn, W. 1973 Fördern. In *Ullmanns Encyklopadie der technischen Chemie*, Vol. 3, pp. 131–184. Chemie, Weinheim.

Nalpanis, P. 1985 Saltating and suspended particles over a flat and sloping surface: II. experiments and numerical simulations. In *Proc. of Int. Workshop on Physics of Blown Sand*, Vol. 1, pp. 37–66, Aarhus University, Denmark.

Ochi, M. 1991 Saltation velocity of the gas–solid two-phase flow in a horizontal pipe. *ASME-FED, Gas–Solid Flows* (Edited by Stock, D. E., Tsuji, Y., Jurewicz, J. T., Reeks, M. W. & Gautam, M.), Vol. 121, pp. 163–166.

Ochi, M. & Ikemori, K. 1978 Minimum transport velocity of granular materials at high concentration in a horizontal pipe. *Bull. JSME* **21,** 1008–1014.

Rizk, F. 1976 Pneumatic conveying at optimal operation conditions and a solution of Barth's equation $\lambda_{\dot{-}} = \phi(\lambda_{\dot{-}}^*, \beta)$. In *Proc. of Pneumotransport 3*, Bedford, U.K., paper D4, pp. 43–58.

Rumpel, D. A. 1985 Successive aeolian saltation: studies of idealized collision. *Sedimentology* **32,** 267–280.

Soo, S. L. 1980 Design of pneumatic conveying systems. *J. Powder Bulk Solids Technol.* **4,** 33–43.

Stegmaier, W. 1978 Zur Berechnung der horizontalen pneumatischen Förderung feinkörniger Feststoffe. *Fördern Heben* **28,** 363–366.

Tsuchiya, Y. 1970 Suggestive saltation of a sand grain by wind. In *Proc. of 12th Coastal Energy Conf., ASCE,* Vol. 3, pp. 1417–1427.

Ungar, J. E. & Haff, P. K. 1987 Steady state saltation in air. *Sedimentology* **34,** 289–299.

Wen, C. Y. & Simons, H. P. 1959 Flow characteristics in horizontal fluidized solids transport. *AIChE Jl* **5,** 263–267.

Werner, B. T. 1990 A steady-state model of wind-blown sand transport. *J. Geol.* **98,** 1–17.

Werner, B. T. & Haff, P. K. 1988 The impact process in aeolian saltation: two-dimensional simulations. *Sedimentology* 35, 320–324.

White, B. R. 1982 Two-phase measurements of saltating turbulent boundary layer flow. *Int. J. Multiphase Flow* **8,** 459–473.

White, B. R. 1986 Particle dynamics in two-phase flows. In *Encyclopedia of Fluid Mechanics*; *Solids and Gas–Solids Flow* (Edited by Cheremisinoff, N. P.), Vol. 4, Chap. 8. Gulf, Houston, TX.

White, B. R. & Schulz, J. C. 1977 Magnus effect in saltation. *J. Fluid Mech.* **81,** 497–512.

Wirth, K.-E. 1983 Critical velocity of solids transport through horizontal circular pipelines. *Ger. Chem. Engng* **6,** 45–52.

Wirth, K.-E. & Molerus, O. 1981 Predictions of pressure drop in horizontal segregated pneumatic conveying with particle strands sliding along the bottom of the pipe. *Ger. Chem. Engng* **4,** 278–284.

Wirth, K.-E. & Molerus, O. 1986 Critical solids transport velocity in horizontal pipelines. In *Encyclopedia of Fluid Mechanics, Solids and Gas–Solids Flow* (Edited by Cheremisinoff, N. P.), Vol. 4, Chap. 11. Gulf, Houston, TX.

Yang, W.-C. 1974 Correlations for solids friction factors in vertical and horizontal pneumatic conveyings. *AIChE Jl* **20,** 605–607.

Zenz, F. A. & Othmer, D. F. 1960 *Fluidization and Fluid–Particle System.* Reinhold, New York.